Journal of Alloys and Compounds 718 (2017) 254–259

Contents lists available at ScienceDirect

Journal of Alloys and Compounds

journal homepage: http://www.elsevier.com/locate/jalcom

Atomic origin for rejuvenation of a Zr-based metallic glass at cryogenic temperature

X.L. Bian [a], G. Wang [a, *], J. Yi [a], Y.D. Jia [a], J. Bednarčík [b], Q.J. Zhai [a], I. Kaban [c], B. Sarac [d], M. Mühlbacher [d], F. Spieckermann [d], J. Keckes [d], J. Eckert [d, e]

[a] Labrotary for Microstructures, Institute of Materials, Shanghai University, Shanghai, 200444, China
[b] DESY Photon Science, Notkestr. 85, 22607, Hamburg, Germany
[c] IFW Dresden, Institute for Complex Materials, Helmholtzstr. 20, 01069, Dresden, Germany
[d] Department Materials Physics, Montanuniversität Leoben, Jahnstraße 12, A-8700, Leoben, Austria
[e] Erich Schmid Institute of Materials Science, Austrian Academy of Sciences, Jahnstraße 12, A-8700, Leoben, Austria

ARTICLE INFO

Article history:
Received 29 January 2017
Received in revised form
24 April 2017
Accepted 12 May 2017
Available online 13 May 2017

Keywords:
Metallic glass
High energy X-ray diffraction
Volume shrinkage
Atomic structural evolution

ABSTRACT

The temperature-dependent atomic structural evolution of a $Zr_{64.13}Cu_{15.75}Ni_{10.12}Al_{10}$ metallic glass is studied by *in-situ* high-energy X-ray diffraction in the temperature range of 79–553 K. The interatomic distance in the first nearest neighbor shell increases with decreasing temperature, while the interatomic distance in other atomic shells decreases. This decrease in the interatomic distances causes volume shrinkage and an increase in the strength of the metallic glass. The volume shrinkage can be quantitatively described by the Varshni function. The structural information is helpful for deeply understanding of the origin of the rejuvenation of metallic glasses at the cryogenic temperatures.

1. Introduction

As a kind of metastable materials, the structure of metallic glasses and the physical properties can be dramatically influenced by external fields, such as force and temperature fields [1]. A further insight into this phenomenon is important to better understand the glass-forming ability, as well as the deformation mechanism and the glass transition behavior etc [2–7]. Thus, the behavior of metallic glasses upon external stress has been extensively studied both experimentally and theoretically, and it is now widely accepted that cluster motifs, corresponding to free volume [8,9], shear transformation zones [10,11], and flow units [12,13], are essentially structural entities operating as strain carriers. More recently, the influence of temperature on the structure and properties of metallic glasses has been investigated extensively [4,5,14–19]. However, these studies focused on the high temperature effects. In contrast, the structural evolution of metallic glasses at low temperatures, e.g. cryogenic temperatures, has not been investigated thoroughly up to date, because the structural evolution at cryogenic temperatures is a reversible process which means that the change in the structure of metallic glasses is very tiny and difficult to be observed. Once the temperature is decreased to a cryogenic level, metallic glasses usually exhibit improved yield strength and enhanced plastic deformability, i.e. a rejuvenation of metallic glasses [20–25], which indicates that metallic glasses are potentially good materials for components used under extreme low temperature conditions. This requires a better understanding of the atomic structural evolution in the low temperature regime to further elucidate the mechanical behavior.

Previous studies have found that besides thermal expansion, a liquid-liquid phase transformation can happen in the atomic clusters of metallic melts [4,14,17], which can cause thermal shrinkage in the first nearest neighbor shell [14]. This contraction in the first shell of metallic melts gives insight into the atomic structure evolution at cryogenic temperatures.

To address this issue, in this work, *in-situ* high energy synchrotron X-ray diffraction (XRD) measurements at cryogenic temperatures are used to analyze the changes in the atomic structure. We choose a $Zr_{64.13}Cu_{15.75}Ni_{10.12}Al_{10}$ (at.%) metallic glass as a model material. This metallic glass has a high glass-forming ability, and its elastic parameters are well known [26]. The aim of this work is to

* Corresponding author.
E-mail address: g.wang@i.shu.edu.cn (G. Wang).

http://dx.doi.org/10.1016/j.jallcom.2017.05.124
0925-8388/

characterize the temperature-dependent structural behavior of the metallic glass, and to correlate cooling shrinkage and elastic properties.

2. Experimental procedure

Alloy ingots were prepared by arc melting a mixture of pure metals (purities higher than 99.99%) in a Ti-gettered high-purity Ar atmosphere, followed by suction casting into copper molds to form rod-like samples (2 mm diameter × 70 mm length, and 1 mm diameter × 30 mm length) and a plate-like sample ($2 \times 10 \times 70$ mm^3). Samples with a length/diameter ratio of 2 were cut from the metallic glass rods by a diamond saw, and the surface roughness of the two parallel ends were polished to 5 μm. The compression tests were carried out at a strain rate of 2.5×10^{-4} s^{-1} in the temperature range of 293–123 K. Details of the experimental setup can be found elsewhere [24,25]. The bulk modulus was measured by a modulus and internal friction analyzer (RFDA MF SYSTEM 21). The specimen for such measurement was $50 \times 10 \times 1$ mm^3, which was conducted in a temperature range of 114–293 K in a JE-LT attachment on the internal friction analyzer by the free vibrational method with a vibrational frequency approximately 1000 Hz.

In-situ XRD experiments were performed at the P02.1 beamline of the PETRA III electron storage ring (DESY Hamburg, Germany). The sample (1 mm diameter × 2 mm length) was held in a quartz capillary with 1.2 mm diameter and 20 μm wall thickness. The diffracted photons were collected using a 2D detector (Perkin Elmer PEI1621) mounted orthogonal to the X-ray beam. The beam size was 0.6×0.6 mm^2 and the wavelength was 0.20727 Å. The sample-to-detector distance and tilting of the image plate detector with respect to the beam axis were calibrated using the diffraction pattern from LaB_6 (NIST 660a). The sample was cooled from ambient temperature down to approximately 79 K, followed by heating from 79 K up to 553 K. The heating/cooling rates were 5 K/min.

3. Results and discussion

The high energy XRD patterns of the $Zr_{64.13}Cu_{15.75}Ni_{10.12}Al_{10}$

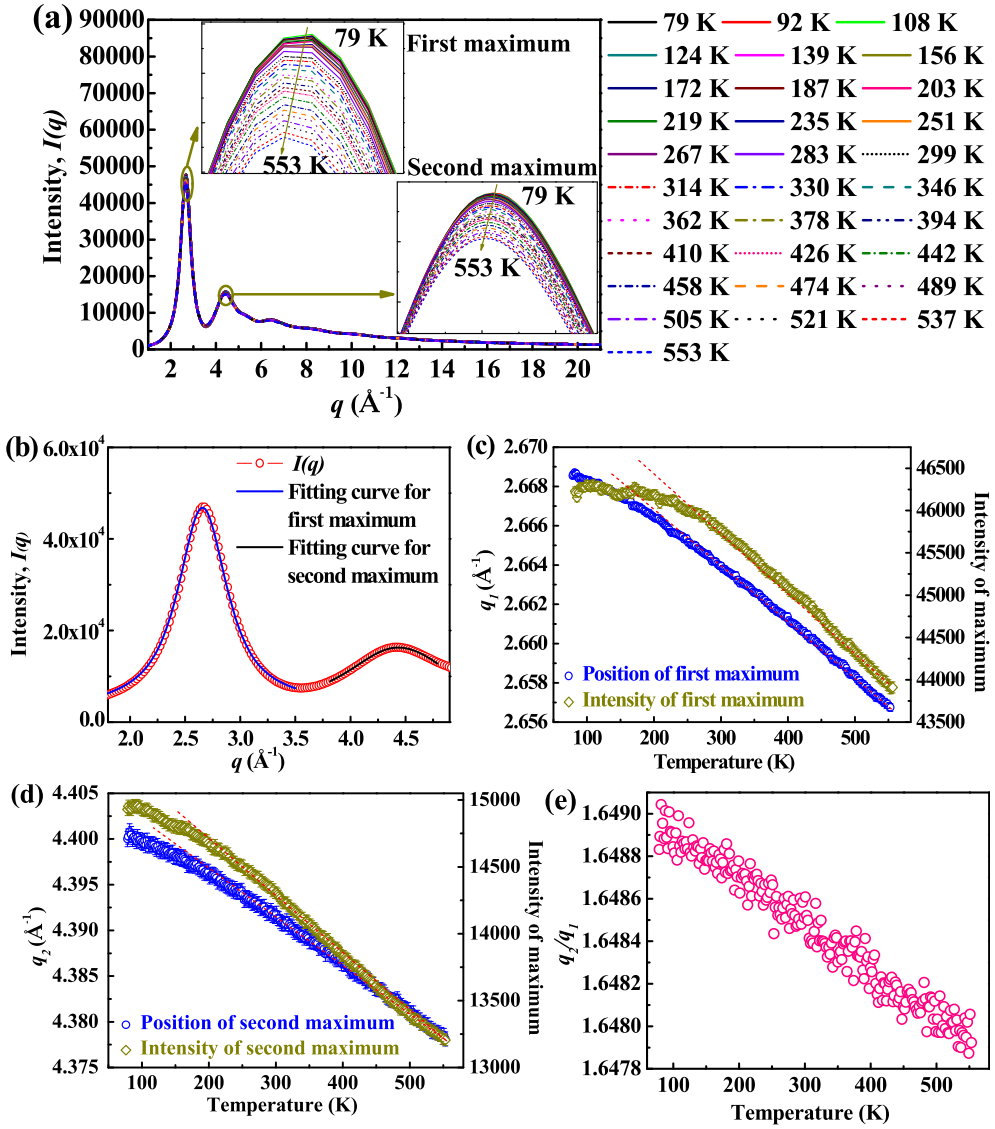

Fig. 1. High energy X-ray diffraction results for the $Zr_{64.13}Cu_{15.75}Ni_{10.12}Al_{10}$ metallic glass. (a) Integrated diffraction curves, $I(q)$, at different temperatures. (b) Enlarged first maximum of a $I(q)$ curve and pseudo-Voigt fits of the maxima. (c) Position, q_1, and intensity, $I(q_1)$, of the first maximum vs. temperature. (d) Position, q_2, and intensity, $I(q_2)$, of the second maximum vs. temperature. (e) Ratio between q_2/q_1 vs. temperature.

metallic glass measured at temperatures from 553 K to 79 K show a fully glassy nature. The intensity curves, $I(q)$, directly integrated from the diffraction patterns are representatively shown in Fig. 1(a). Decreasing the temperature does not significantly change the structure of the glass. Detailed view of the first and second maxima in the $I(q)$ curves at different temperatures reveals that the intensity and the peak position slightly change with decreasing temperature [see the insets in Fig. 1(a)]. Since the first maximum of the $I(q)$ curve corresponds to the medium-range order (MRO) in the glassy phase, and the maximum at higher q values reflects the structural information from the next nearest neighbor shell [27], it is necessary to further quantitatively investigate the changes of the maxima as functions of temperature.

To reveal the information hidden in the maxima of the $I(q)$ curves, a pseudo-Voigt function was used to fit the peaks. Fig. 1(b) clearly shows that the pseudo-Voigt function can perfectly fit the first and second maxima in the $I(q)$ curve, from which the scattering intensity and the positions of the maxima can be plotted as the functions of temperature [Fig. 1(c) and (d)]. The positions of both the first and the second maximum, q_1 and q_2, shift to higher values, corresponding to a contraction in the interatomic distances with decreasing temperature. In the temperature range from 553 K to approximately 220 K, both the position of the two maxima and their intensity follow a linear trend [see Fig. 1(c) and (d)]. However, further decreasing the temperature, these temperature dependences become non-linear. It is interesting that the ratio of q_2/q_1 exhibits an increasing trend with decreasing temperature as shown in Fig. 1(e). This suggests that the structural changes, in particular shrinkage, occur in the different atomic shells with decreasing temperature, i.e. they are inhomogeneous.

According to the Debye equation [28], decreasing temperature should result in a cooling shrinkage in a homogeneous manner. The intensity of the diffraction pattern of the glassy phase, $I(q)$, can be described by:

$$I(q) = \sum f_i f_j \frac{\sin(qr_{ij})}{qr_{ij}} \quad (1)$$

where f_i and f_j are the atom form factors and r_{ij} are the interatomic distances ($i, j = 1, \ldots, n$). By homogeneous structural changes, all interatomic distances r_{ij} should decrease with temperature by the same factor, i.e., $r_{ij}(T) = r_{ij}(1\text{-}\alpha\cdot\Delta T) = r_{ij}\cdot k$, and the scattered intensity $I^*(q/k)$ is equal to $I(q)$. This means that the positions of the maxima q^*_i of the scattering functions of $I^*(q)$ are decreased by a factor $1/k$. Hence, the ratio of the positions of any two maxima in the $I(q)$ curves should change constantly with decreasing temperature. However, Fig. 1(e) clearly shows an inhomogeneous shrinkage in different atomic shells.

To further characterize the different changes in different shells, the pair distribution functions ($g(r)$) in real space were investigated [Fig. 2(a)]. The enlarged first maximum shows that the position shifts to higher r values with decreasing temperature, while reverse change occurs for the second maximum [see the inset in Fig. 2(a)]. And Gaussian fitting of the first maximum (see Fig. 2(b)) also reveals that the position of the first maximum almost linearly increases with decreasing temperature, as shown in Fig. 2(c). Hence, the first atomic shell expands unexpectedly upon cooling. In contrast, the position of the second maximum at different temperatures shifts to lower r values [see Fig. 2(c)], which is consistent with the results following from the $I(q)$ curves in Fig. 1, i.e. a cooling shrinkage occurs in the higher atomic shells of the metallic glass [24].

The above findings indicate inhomogeneous shrinkage of the metallic glass at the atomic scale. The atoms in the higher coordination shells, i.e., at the medium-range scale, shrink with decreasing temperature [Fig. 1(c) and (d)]. While the interatomic distance of the first shell increases, causing the position of the first maximum to shift to higher r values in the $g(r)$ curve [Fig. 2(c)]. This

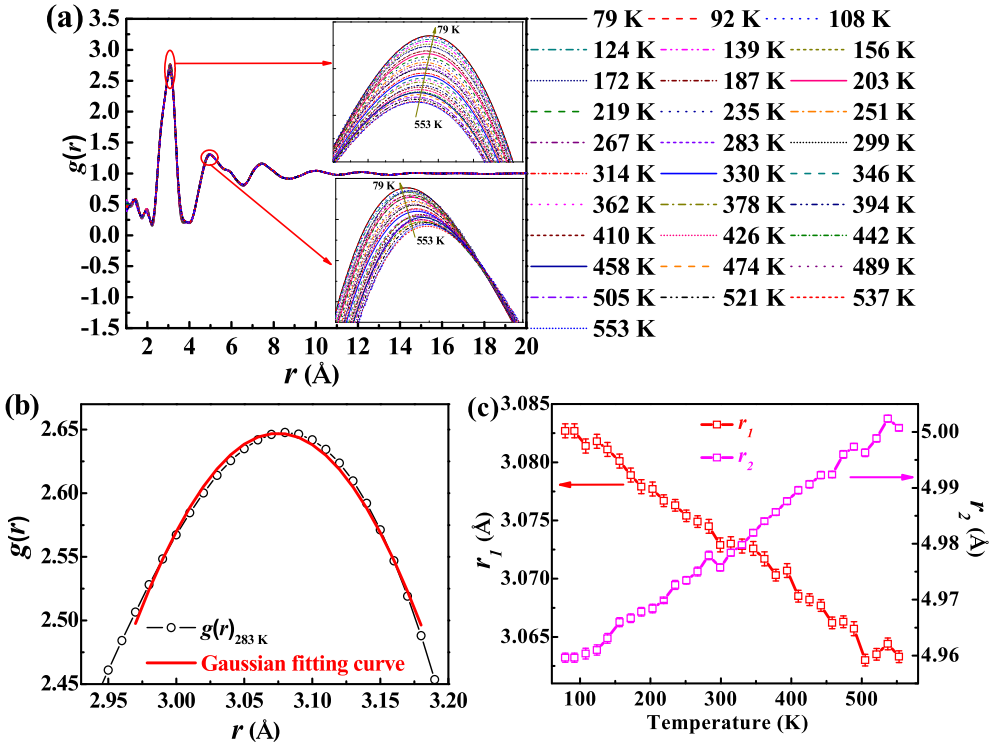

Fig. 2. (a) Pair distribution function, $g(r)$, of the $Zr_{64.13}Cu_{15.75}Ni_{10.12}Al_{10}$ metallic glass at different temperatures. The insets show the enlarged first and second maxima. (b) Sketch of Gaussian fitting the first maximum in the $g(r)$ curve at the temperature of 283 K. (c) The position values of the first maximum (r_1) and the second maximum (r_2) versus temperature.

unexpected expansion of the first atomic shell is suggested to be ascribed to a highly spatially localized process of atomic rearrangement around the large Zr solvent atoms with decreasing temperature [24].

Since the $I(q)$ curve corresponds to reciprocal space, one can roughly use the first and the second maxima to reflect the evolution in the MRO and the next nearest neighbor shells, respectively [29]. The shift of the maxima in the $I(q)$ curve corresponds to the change in interatomic distance, which further causes atomic volume changes in the glassy phase in the MRO and the next nearest neighbor shells. According to the q_1 and q_2 shifts, the volume changes, ΔV, in the MRO and the next nearest neighbor shells can be estimated by $\Delta V = (q_{nR}^3 - q_{nT}^3)/q_{nR}^3$ $(n = 1, 2)$, where q_{nT} is the position of the maxima at different temperatures and q_{nR} is the position of the maxima at room temperature of 293 K. The temperature dependences of the volume changes $\Delta V = f(T)$ for the $Zr_{64.13}Cu_{15.75}Ni_{10.12}Al_{10}$ metallic glass is depicted in Fig. 3(a). It can be seen that the volume changes ΔV^I and ΔV^{II} calculated from the positions of the first and the second maxima do not coincide. Similar to changes of the peak positions shown in Fig. 1, both temperature dependences are virtually linear in the temperature range from 553 to 220 K and become non-linear at lower temperatures.

In solids, the volume depends on the frequency of lattice vibration, and the coefficient of thermal expansion is proportional to the lattice specific heat [30,31]. As such, the enthalpy of a solid, which is an integral of the lattice specific heat, is proportional to the temperature dependent volume change, ΔV. The lattice specific heat of a solid in a wide temperature range is usually described by the Einstein model [32]. In this case, the volume change, ΔV, due to the temperature change can be can be universally modeled by the Varshni expression [33]:

$$\Delta V = \Delta V_0 - \frac{S}{\exp(\theta/T) - 1}, \quad (2)$$

where ΔV_0 is the volume change at 0 K, and θ and S are the effective Einstein temperature and an adjustable parameter related to the strength of the anharmonic interactions [34], respectively. The fitting parameters are also given in Fig. 3(a). The maximum volume shrinkage values at 0 K, ΔV_0, deduced from the first and the second maximum are 5.01×10^{-3} and 5.65×10^{-3}, i.e. they differ by 11%. This further confirms that non-homogeneous shrinkage occurs in different atomic shells.

The volume shrinkage must influence the elastic properties of the metallic glass because the interatomic distance is compressed [34,35]. Fig. 3(b) shows that the bulk modulus, K, of the $Zr_{64.13}Cu_{15.75}Ni_{10.12}Al_{10}$ metallic glass monotonically increases with decreasing temperature. Based on the $I(q)$ and $g(r)$ curves (Figs. 1 and 2), it can be rationalized that the inhomogeneously thermal

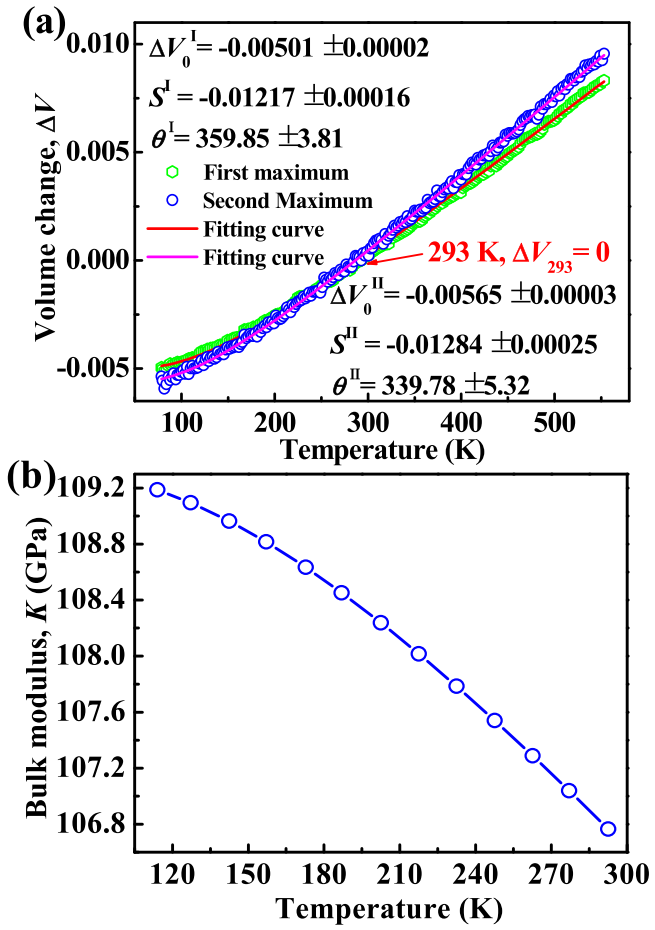

Fig. 3. (a) Volume changes due to contraction at low temperatures, estimated from the shifts of the positions of the first and second maxima of the $I(q)$ curve. The Varshni function fitting curves (lines) are plotted and the fitting parameters are also listed. (b) Bulk modulus of the $Zr_{64.13}Cu_{15.75}Ni_{10.12}Al_{10}$ metallic glass as a function of temperature.

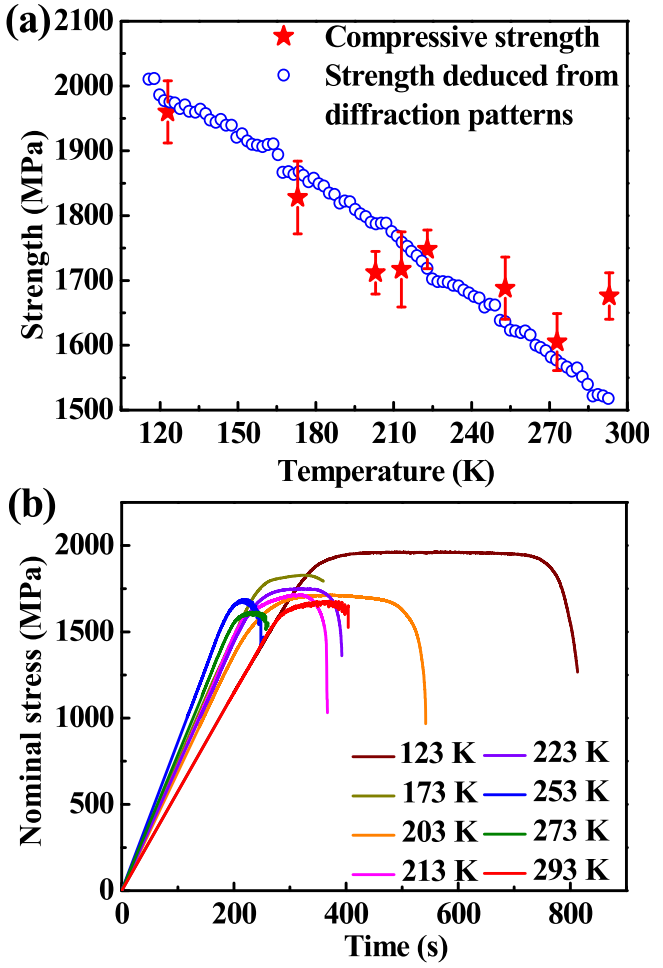

Fig. 4. Compressive curves and strength of the $Zr_{64.13}Cu_{15.75}Ni_{10.12}Al_{10}$ metallic glass vs. temperature. (a) Maximum compressive strength deduced from the volume shrinkage. For comparison, experimental values are also plotted (marked as stars). (b) Stress-time curves at different temperatures.

expansion of the metallic glass takes place, which is expected to introduce thermal stresses [20]. With decreasing temperature, the interatomic distance is compressed, and it needs an extra stress to compensate this change to be an equilibrium state. According to the linearly thermal expansion coefficient of 1.0×10^{-5} K^{-1} [19], the linearly thermal strain due to the cooling effect from 293 K to 77 K is evaluated to be approximately 0.2%, which would induce the internal stress to be 10% of the macroscopic yield stress [20]. However, this evaluated internal stress is lower than the experimental value (~20% of the yield stress), which is possible due to the inhomogeneously thermal expansions in different structural motifs, i.e., thermal expansion in MRO and thermal shrinkage in the first nearest neighbor shell. According to the concept of concordant region [35], when the atoms in the first nearest neighbor shell move, the local stress will be changed [35], which then causes that the surrounding atoms in MRO concordantly shift to counterbalance the changes in the local stress. Thus, a stress increment is formed. In the present study, the thermal shrinkage in the first shell and the thermal expansion in other shells could be treated as a concordantly shifting region. Therefore, the stress increment, Δp, due to the movement of atoms in the concordantly shifting region is generated. Such stress increment involving volume change is associated with the bulk modulus, i.e., $\Delta p = K \cdot \Delta V$ [34]. The bulk modulus is a macroscopic manifestation of atomic bonding, which is directly related to the external forces required to compress or extend the interatomic distance in opposition to the internal forces that seek to establish equilibrium interatomic distance [34].

Accordingly, multiplying the volume change values extracted from the first maximum with the bulk modulus, one can obtain the stress increment versus temperature, as shown in Fig. 4(a). It is evident that the volume shrinkage causes the stress increment to approach 592 MPa when the temperature decreases from room temperature to 115 K. To find the correlation between this stress increment and the macroscale behavior, we conducted compression tests at different temperatures (from 293 K to 123 K) with a strain rate of 2.5×10^{-4} s^{-1}. The compressive nominal stress-time curves are shown in Fig. 4(b). The curves demonstrate that the compressive strength increases with decreasing test temperature [22–25]. The yield strength of the $Zr_{64.13}Cu_{15.75}Ni_{10.12}Al_{10}$ metallic glass at room temperature is around 1518 MPa. The method to determine the yield strength can be found in Ref. [36]. We use this strength (1518 MPa) as the starting point and add the stress increment to this original value. This allows predicting the strength change with decreasing temperature and to compare it with the experimentally values determined from the compression tests [Fig. 4(a)]. Apparently, the strength values predicted from the volume shrinkage and the bulk modulus change agrees well with the experimental values. Compared to that at the room temperature, the metallic glass cooled to cryogenic temperatures is compressed by the stress increment. Upon compression, the external stress must firstly compensate this stress increment. Moreover, a complex hierarchical structure of shear-branching process as well as large activation energy of the shear transformation zone will be formed due to the inhomogeneous thermal contraction at low temperatures [37]. Thus, the yield strength is enhanced.

4. Conclusions

In summary, decreasing the temperature to the cryogenic level causes volume contraction in the $Zr_{64.13}Cu_{15.75}Ni_{10.12}Al_{10}$ metallic glass. This volume shrinkage can be quantitatively described by the Varshni function reflecting the atomic changes in the medium range. The volume shrinkage is correlated with the displacement of atoms in the first nearest neighbor shell, and the increase of the interatomic distance in the first nearest neighbor shell. The results offer a structural picture for understanding the increase in bulk modulus and strength with decreasing temperature.

Acknowledgments

The authors would like to acknowledge the financial support from the National Key Basic Research Program from MOST (No. 2015CB856800), the NSFC (Grant Nos. 51671120 and 51501106), the 111 project, the China Postdoctoral Science Foundation (No. 2016M601563) and the Natural Science Foundation of Shanghai (No. 17ZR1440800). Parts of this research were carried out at the light source PETRA III (beamline P02.1) at DESY, a member of the Helmholtz Association (HGF). Additional support through the DFG Leibniz Program (grant EC 111/26-1) and the European Research Council under the ERC Advanced Grant INTELHYB (grant ERC-2013-ADG-340025), as well as stimulating discussions with L.B. Bruno, K.G. Prashanth and D. Şopu are gratefully acknowledged.

References

[1] C.A. Schuh, T.C. Hufnagel, U. Ramamurty, Mechanical behavior of amorphous alloys, Acta Mater. 55 (2007) 4067–4109.
[2] P.G. Debenedetti, F.H. Stillinger, Supercooled liquids and the glass transition, Nature 410 (6825) (2001) 259–267.
[3] C. Tang, P. Harrowell, Anomalously slow crystal growth of the glass-forming alloy CuZr, Nat. Mater. 12 (6) (2013) 507–511.
[4] S. Wei, F. Yang, J. Bednarcik, I. Kaban, O. Shuleshova, A. Meyer, R. Busch, Liquid-liquid transition in a strong bulk metallic glass-forming liquid, Nat. Commun. 4 (2013) 2083.
[5] K.F. Kelton, G.W. Lee, A.K. Gangopadhyay, R.W. Hyers, T.J. Rathz, J.R. Rogers, M.B. Robinson, D.S. Robinson, First x-ray scattering studies on electrostatically levitated metallic liquids: demonstrated influence of local icosahedral order on the nucleation barrier, Phys. Rev. Lett. 90 (19) (2003) 195504.
[6] H.W. Sheng, W.K. Luo, F.M. Alamgir, J.M. Bai, E. Ma, Atomic packing and short-to-medium-range order in metallic glasses, Nature 439 (7075) (2006) 419–425.
[7] D. Ma, A.D. Stoica, X.L. Wang, Z.P. Lu, B. Clausen, D.W. Brown, Elastic moduli inheritance and the weakest link in bulk metallic glasses, Phys. Rev. Lett. 108 (8) (2012) 085501.
[8] F. Spaepen, A microscopic mechanism for steady state inhomogeneous flow in metallic glasses, Acta Metall. 25 (4) (1977) 407–415.
[9] J.C. Ye, J. Lu, C.T. Liu, Q. Wang, Y. Yang, Atomistic free-volume zones and inelastic deformation of metallic glasses, Nat. Mater. 9 (8) (2010) 619–623.
[10] A.S. Argon, Plastic deformation in metallic glasses, Acta Metall. 27 (1) (1979) 47–58.
[11] D.B. Miracle, A structural model for metallic glasses, Nat. Mater. 3 (10) (2004) 697–702.
[12] Z. Lu, W. Jiao, W.H. Wang, H.Y. Bai, Flow unit perspective on room temperature homogeneous plastic deformation in metallic glasses, Phys. Rev. Lett. 113 (4) (2014) 045501.
[13] Z. Wang, B.A. Sun, H.Y. Bai, W.H. Wang, Evolution of hidden localized flow during glass-to-liquid transition in metallic glass, Nat. Commun. 5 (2014) 5823.
[14] H. Lou, X. Wang, Q. Cao, D. Zhang, J. Zhang, T. Hu, H.K. Mao, J.Z. Jiang, Negative expansions of interatomic distances in metallic melts, Proc. Natl. Acad. Sci. U. S. A. 110 (25) (2013) 10068–10072.
[15] Y.T. Shen, T.H. Kim, A.K. Gangopadhyay, K.F. Kelton, Icosahedral order, frustration, and the glass transition: evidence from time-dependent nucleation and supercooled liquid structure studies, Phys. Rev. Lett. 102 (5) (2009) 057801.
[16] V.V. Vasisht, S. Saw, S. Sastry, Liquid–liquid critical point in supercooled silicon, Nat. Phys. 7 (7) (2011) 549–553.
[17] N. Jakse, L. Hennet, D.L. Price, S. Krishnan, T. Key, E. Artacho, B. Glorieux, A. Pasturel, M.L. Saboungi, Structural changes on supercooling liquid silicon, Appl. Phys. Lett. 83 (23) (2003) 4734–4736.
[18] N. Mattern, M. Stoica, G. Vaughan, J. Eckert, Thermal behaviour of $Pd_{40}Cu_{30}Ni_{10}P_{20}$ bulk metallic glass, Acta Mater. 60 (2012) 517–524.
[19] X. Tong, G. Wang, Z.H. Stachurski, J. Bednarčík, N. Mattern, Q.J. Zhai, J. Eckert, Structural evolution and strength change of a metallic glass at different temperatures, Sci. Rep. 6 (2016) 30876.
[20] S.V. Ketov, Y.H. Sun, S. Nachum, Z. Lu, A. Checchi, A.R. Beraldin, H.Y. Bai, W.H. Wang, D.V. Louzguine-Luzgin, M.A. Carpenter, A.L. Greer, Rejuvenation of metallic glasses by non-affine thermal strain, Nature 524 (7564) (2015) 200–203.
[21] H. Li, C. Fan, K. Tao, H. Choo, P.K. Liaw, Compressive behavior of a Zr-Based metallic glass at cryogenic temperatures, Adv. Mater. 18 (6) (2006) 752–754.
[22] Z.Y. Liu, G. Wang, K.C. Chan, J.L. Ren, Y.J. Huang, X.L. Bian, X.H. Xu, D.S. Zhang, Y.L. Gao, Q.J. Zhai, Temperature dependent dynamics transition of intermittent plastic flow in a metallic glass. I. Experimental investigations, J. Appl.

Phys. 114 (3) (2013) 033520.
[23] D. Klaumünzer, A. Lazarev, R. Maass, F.H. Dalla Torre, A. Vinogradov, J.F. Löffler, Probing shear-band initiation in metallic glasses, Phys. Rev. Lett. 107 (18) (2011) 185502.
[24] X.L. Bian, G. Wang, Q. Wang, B.A. Sun, I. Hussain, Q.J. Zhai, N. Mattern, J. Bednarčík, J. Eckert, Cryogenic-temperature-induced structural transformation of a metallic glass, Mater. Res. Lett. 5 (4) (2017) 284–291.
[25] Y.W. Wang, X.L. Bian, S.W. Wu, I. Hussain, Y.D. Jia, J. Yi, G. Wang, Rate dependent of strength in metallic glasses at different temperatures, Sci. Rep. 6 (2016) 27747.
[26] Y.H. Liu, G. Wang, R.J. Wang, D.Q. Zhao, M.X. Pan, W.H. Wang, Super plastic bulk metallic glasses at room temperature, Science (New York, N.Y.) 315 (5817) (2007) 1385–1388.
[27] N. Mattern, J. Bednarčik, S. Pauly, G. Wang, J. Das, J. Eckert, Structural evolution of Cu–Zr metallic glasses under tension, Acta Mater. 57 (14) (2009) 4133–4139.
[28] P. Debye, Zerstreuung von Röntgenstrahlen, Ann. Phys. 351 (6) (1915) 809–823.
[29] G. Wang, N. Mattern, J. Bednarčík, R. Li, B. Zhang, J. Eckert, Correlation between elastic structural behavior and yield strength of metallic glasses, Acta Mater. 60 (6–7) (2012) 3074–3083.
[30] J. Fabian, P.B. Allen, Thermal expansion and grüneisen parameters of amorphous silicon: a realistic model calculation, Phys. Rev. Lett. 79 (10) (1997) 1885–1888.
[31] L.M. Thomas, J. Shanker, Temperature dependence of elastic constants and thermal expansion coefficient for NaCl crystals, Phys. Stat. Sol. (b) 195 (1996) 361–366.
[32] A. Einstein, Die Plancksche Theorie der Strahlung und die Theorie der spezifischen Wärme, Ann. Phys. 327 (1) (1907) 180–190.
[33] Y.P. Varshni, Temperature dependence of the elastic constants, Phys. Rev. B 2 (1970) 3952.
[34] W.H. Wang, The elastic properties, elastic models and elastic perspectives of metallic glasses, Prog. Mater. Sci. 57 (3) (2012) 487–656.
[35] K. Trachenko, Slow dynamics and stress relaxation in a liquid as an elastic medium, Phys. Rev. B 75 (2007) 212201.
[36] X.L. Bian, G. Wang, H.C. Chen, L. Yan, J.G. Wang, Q. Wang, P.F. Hu, J.L. Ren, K.C. Chan, N. Zheng, A. Teresiak, Y.L. Gao, Q.J. Zhai, J. Eckert, J. Beadsworth, K.A. Dahmen, P.K. Liaw, Manipulation of free volumes in a metallic glass through Xe-ion irradiation, Acta Mater. 106 (2016) 66–77.
[37] C. Chen, J. Ren, G. Wang, K.A. Dahmen, P.K. Liaw, Scaling behavior and complexity of plastic deformation for a bulk metallic glass at cryogenic temperatures, Phys. Rev. E, Stat. Nonlinear, Soft Matter Phys. 92 (1) (2015) 012113.